

---

# Geometry-aware Transformer for molecular property prediction

---

**Bumju Kwak**

Recommendation Team  
Kakao Corporation  
Gyeonggi, Republic of Korea  
meson3241@gmail.com

**Jeonghee Jo**

Institute of New Media and Communications  
Seoul National University  
Seoul 08826, Republic of Korea  
page1024@snu.ac.kr

**Byunghan Lee**

Department of Electronic Engineering  
Seoul National University of Science and Technology  
Seoul 01811, Republic of Korea  
bhlee@seoultech.ac.kr

**Sungroh Yoon**

Department of Electrical and Computer Engineering  
Seoul National University  
Seoul 08826, Republic of Korea  
sryoon@snu.ac.kr

## Abstract

Recently, message passing neural networks (MPNNs) have achieved remarkable performances for various chemical tasks. However, the message passing scheme can only cover a local field, and cannot capture long-range relationship between atoms. This behavior does not accord with chemical theory, which is one of the fundamental limitations of the MPNNs. In this work, we propose a novel Transformer-based framework for representation learning on molecules, named Geometry-aware Transformer (GeoT). GeoT learns sequential representations of molecule graphs based on global attentions. By virtue of the Transformer-based architecture and additional refinements, the smoothing problem can be significantly alleviated compared to graph convolution-based architectures. GeoT achieved comparable performances with other recent MPNN-based models. We also verified the intuition behind GeoT with respect to the reasonability and interpretability, through attention visualization.

## 1 Introduction

Quantum mechanical (QM) calculations have been used for development of chemicals in various fields, such as drugs, catalysts, or novel industrial materials. Density functional theory (DFT) is the most widely used computational modeling method used for modern QM research. However, DFT requires tremendous computations to predict properties for a small molecule.

For this reason, several machine learning-based methods have been developed to replace DFT calculation with more cost-effective alternatives [1, 2, 3, 4]. Motivated by recent advances in deep learning, many recent models [5, 6, 7, 8, 9, 10, 11] adopted deep learning-based methods to predict various molecular properties including energy and forces.

Message passing neural network (MPNN) [12] is one of the most widely used frameworks for graph neural networks (GNNs) in recent days. In these kinds of works, a molecule is described as a graph, and its atoms are represented as discrete nodes scattered in Euclidean space. These models do not consider any bond type information. Instead, they construct edges between all node pairs located within the fixed cutoff distance from each other. Then, the message passing layers do a graph convolution with each atom and its local substructures (messages) which are controlled by radial basis filters. Many atomistic models [6, 12, 7, 13] based on MPNN showed competitive performances in various QM tasks.

Although promising performances on existing MPNNs, there are several fundamental limitations in the localized view. In theory, every atom pair in a molecule has their own interaction defined by their charges and distance. In other words, atom-atom interactions exist over a broad range in the molecule. Therefore, all atom-atom interactions should be considered properly in molecular property prediction models regardless of their distances. However, the localized convolutions of MPNN have conflict with this conformational behavior of molecules, since MPNN with a finite cutoff value assumes that messages are transferred within a restricted region. It means that MPNN cannot identify any interatomic relationship between atom pairs located outside the cutoff distance from each other. Consequently, MPNNs fail to capture long-range interatomic relationships, which is not a desired property of molecular representation.

Furthermore, the MPNN models are vulnerable to over-smoothing problem [14], which is caused by inherent Laplacian-smoothing effects of message passing. The atom features cannot be distinguished from each other, because the message-passing updates an atom feature by mixing its neighbors in every step. Recent studies [14, 15, 16] reported that the over-smoothing restricts the performance of deep GNNs in various tasks including molecular dataset.

To address the above issues, we developed a novel geometry-aware Transformer (GeoT) consisting of softmax-free attentions, for reasonable structure representation combined with a global view. We removed the positional encoding and introduced radial basis functions (RBFs) to reflect a complete molecular structure and ensuring the permutation invariance of a molecular sequence. We adopted several modifications and refinements to the original self-attention, for enhancing the performance and preventing from the over-smoothing problem.

We summarize our contributions as below.

- We propose a Transformer-based architecture GeoTransformer for molecular graphs, incorporating radial basis embeddings of molecular conformations.
- GeoT is simple yet effective, by capturing global three dimensional structure with less over-smoothing problem. In addition, GeoT provides an intuitive interpretation of atom-atom interactions via the attention values with a global view.
- GeoT achieved competitive performances in various types of benchmarks. Furthermore, we adopted several model refinement tricks to GeoT and analyzed effects thereof.

## 2 Related Works

### 2.1 Graph neural networks for molecules

The molecular representation as a graph has been widely used from early stages. These methods regard a molecule as a graph consisting of discrete atom nodes with bonds as edges. BPNN [3] is the first neural network model which calculates energy from molecular graphs. The first work using graph convolution on molecules [5] trained each atom representation with localized filters. GDML [17, 18, 19] used conservative force fields of each atom, and MPNN [12] proposed message passing framework for local update of each atom representation in the network.

SchNet [6], PhysNet [7] and several MPNN-based models constructed localized messages centered on atoms with continuous filters based on interatomic distances. More recent works such as DimeNet [10], DimeNet++ [13], GemNet [20], and SphereNet [21] compute angles to describe molecular conformations more concretely. Some works like TFN [22], Cormorant [8], and SE(3)-Transformer [23] adopt group equivariances in their models to preserve roto-translational symmetry. These previous models need a cutoff value in common, which restricts the receptive field of an atom-wise

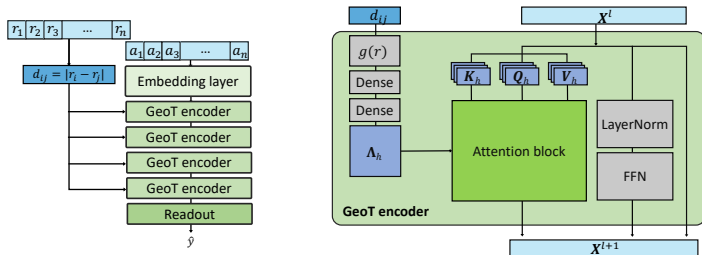


Figure 1: Overall architecture of Geometry-aware Transformer

convolution. In addition, these previous methods depends on tremendous computations for geometric embedding for embedding explicit equivariences.

## 2.2 Self-attention and Transformer on molecular graphs

The self-attention has been widely adopted for learning sequential data, because it can capture the relations between two components from the sequence. Transformer [24] is a type of encoder-decoder architecture with a stack of self-attention layers, to efficiently handle sequential data such as sentences regardless of their lengths. We also applied AttnScale [25] and other strategies for effective implementation of the attention mechanism on graphs.

For molecular property prediction tasks, Transformer-like structures have been used for sequential representation of molecules such as SMILES [26], rather than graph-structured form. MAT [27] and GRAT [9] used a self-attention on molecular graphs, whereas the distance representations between atom pairs of their model were incomplete to capture long-range interactions. Recently, [28, 29, 30], which are another Transformer-based models with a global view of attention. However, they only count hops between two nodes rather than real geometric distances.

## 3 Preliminary

### 3.1 Notation

We denote a molecule as a set of  $N$  atoms  $\{a_i\}_{i \in \{1, \dots, N\}}$  with coordinates  $\{\mathbf{r}_i\} \in \mathbb{R}^3$ . We calculate the Euclidean distance  $r_{ij} = \|\mathbf{r}_i - \mathbf{r}_j\|_2$  between two atom  $a_i$  and  $a_j$ . Our model is a stack of  $L$  layers, which transforms input  $\mathbf{X}^l$  into output  $\mathbf{X}^{l+1}$ , especially the first layer input  $\mathbf{X}^0$  is given from embedding layer which only depends on atomic number.

### 3.2 Transformer encoder

#### 3.2.1 Multi-head self attention (MSA)

For given set of vectors  $\{\mathbf{X}_i^l\}_{i \in \{1, \dots, N\}}$ , MSA is calculated by incorporating vectors using weight called *self-attention*, which represents interaction between  $\mathbf{X}_i^l$  and  $\mathbf{X}_j^l$ . Self-attention first transforms input feature  $\mathbf{X}$  into three types of tensors, query  $\mathbf{Q}$ , key  $\mathbf{K}$ , and value  $\mathbf{V}$ , respectively. Each matrices are obtained by multiplication of trainable weights  $W_Q, W_K, W_V$ .

$$\mathbf{Q} = W_Q \mathbf{X}, \quad \mathbf{K} = W_K \mathbf{X}, \quad \mathbf{V} = W_V \mathbf{X} \quad (1)$$

With  $\mathbf{Q}$ ,  $\mathbf{K}$ , and  $\mathbf{V}$ , self-attention yields weighted sum of  $\mathbf{V}$ , which weights are given by scaled dot-product between  $\mathbf{Q}$  and  $\mathbf{K}$  scaled by vector dimension  $d_m$ .

$$\text{Attention}(\mathbf{Q}, \mathbf{K}, \mathbf{V}) = \text{softmax}(\mathbf{Q}\mathbf{K}^T / \sqrt{d_m}) \cdot \mathbf{V} \quad (2)$$

MSA [24] was proposed to improve model performance instead of using single self-attention only. For MSA,  $\{\mathbf{Q}, \mathbf{K}, \mathbf{V}\}$  are split into  $h$  matrices  $\{\mathbf{Q}_i, \mathbf{K}_i, \mathbf{V}_i\}_{i \in \{1, \dots, h\}}$  with dimension  $d_m/h$ . Self-attention is then applied to  $\{\mathbf{Q}_i, \mathbf{K}_i, \mathbf{V}_i\}_{i \in \{1, \dots, h\}}$ , followed by concatenation.

$$\begin{aligned} \mathbf{H}_i &= \text{Attention}(\mathbf{Q}_i, \mathbf{K}_i, \mathbf{V}_i) \quad i \in \{1, \dots, h\} \\ \text{MSA}(\mathbf{X}) &= \text{Concat}(\mathbf{H}_1, \dots, \mathbf{H}_h) \end{aligned} \quad (3)$$

### 3.2.2 Transformer encoder layer

In the Transformer encoder [24] layer, the output from MSA( $\mathbf{X}^l$ ) added to original input  $\mathbf{X}^l$  by residual connection accompanied by layer normalization [31]. After that, the last output  $\tilde{\mathbf{X}}^l$  fed into feed forward network (FFN), consisting of two linear transformations with an ELU [32] activation. Finally, another layer normalization is applied to the output from FFN added by  $\tilde{\mathbf{X}}^l$ .

$$\begin{aligned} \tilde{\mathbf{X}}^l &= \text{LayerNorm}(\text{MSA}(\mathbf{X}^l) + \mathbf{X}^l) \\ \mathbf{X}^{l+1} &= \text{LayerNorm}(\text{FFN}(\tilde{\mathbf{X}}^l) + \tilde{\mathbf{X}}^l) \end{aligned} \quad (4)$$

## 4 Geometry-aware Transformer

We propose GeoT architecture to solve chemical property prediction task with capturing global perspective of a molecule structure. GeoT is built based on consecutive Transformer encoders, with modification for capturing geometric information in Euclidean space.

Geometry-aware Transformers create distance embeddings expanded by multiple RBFs. The embeddings from RBFs are merged with query  $\mathbf{Q}$  and key  $\mathbf{K}$ , which yields geometry-aware attention. GeoT is achieved by calculating weighted sum of the values  $\mathbf{V}$  with weights given from geometry-aware attention. At the end of layer, the readout layer produces predicted graph labels.

### 4.1 Two-body kernel

GeoT adopt distance information by two-body kernel  $\Lambda : [1, \dots, N] \times [1, \dots, N] \rightarrow \mathbb{R}$  with its matrix representation  $\mathbf{\Lambda}$ . To construct  $\mathbf{\Lambda}$ , we define multiple RBFs  $\mathbf{g}(r) : \mathbb{R} \rightarrow \mathbb{R}^{d_m}$  with distances between atom pairs. Many previous studies suggested different types of radial basis functions for these distances [6, 7, 13, 8]. We selected multiple different Gaussian basis functions for RBFs, proposed in SchNet [6] followed by concatenation, where  $\gamma = 10$  adjusts the scales of distance representations and  $\delta = 0.1 \text{ \AA}$  is multiplier.

$$\mathbf{g}(r)_k = \exp(-\gamma||r - \delta k||^2) \quad (5)$$

With  $\mathbf{g}(r)_k$ , we created two-body kernel  $\Lambda^n$  depending distance  $r$  with two-layer multilayer perceptron (MLP)  $f^n$  as follows.

$$\Lambda^n(r) = f^n(\mathbf{g}(r)) \quad (6)$$

Since atomic interaction not only depends on distance between two atoms but their atomic numbers, it is natural to combine atomic number information with distance information  $\mathbf{g}(r)$  to describe two-body interaction between atoms. For this reason, we added vector representation  $Z^n$  of two atom  $a_i$  and  $a_j$  symmetrically to  $\mathbf{g}(r)$ . The two-body kernels are created and trained in each layer individually.

$$\begin{aligned} \mathbf{g}_{\text{emb}}(r_{ij}, a_i, a_j) &= \mathbf{g}(r_{ij}) \oplus (Z^n(a_i) + Z^n(a_j)), Z^n : \mathbb{N} \rightarrow \mathbb{R}^{d_{\text{emb},2}} \\ \Lambda_{ij}^n &= f_{\text{emb}}^n(\mathbf{g}_{\text{emb}}(r_{ij}, a_i, a_j)) \end{aligned} \quad (7)$$

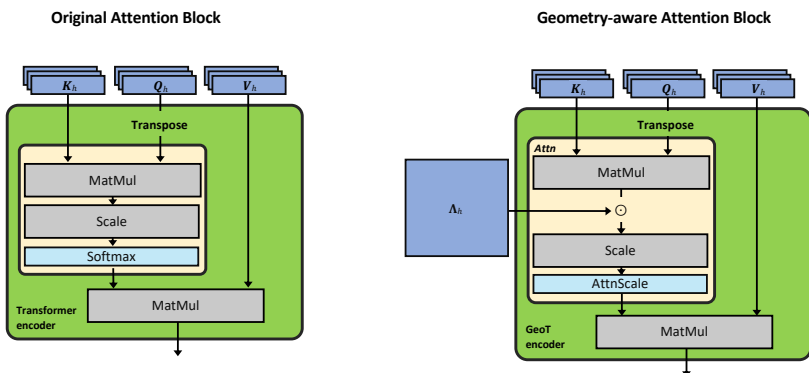


Figure 2: Comparison between the original Transformer and Geometry-aware Transformer. The key differences of two architectures are that the Geometry-aware Transformer 1) adopted the radial basis functions to represent distances of atom pairs, and 2) removed softmax function existed in the original Transformer.

## 4.2 Geometry-aware self-attention

Note that we did not use the standard self-attention in our model. Our Geometry-aware self-attention is different from the standard self-attention in two points: 1) inserting two-body kernel matrix  $\Lambda$  and 2) the absence of softmax operation. In details, we replaced the original attention  $Attn(\mathbf{Q}, \mathbf{K}) = (\mathbf{Q}\mathbf{K}^T)/\sqrt{d_m}$  in Eq. 3 with geometry-aware attention  $Attn_G(\mathbf{Q}, \mathbf{K}, \Lambda) = (\mathbf{Q}\mathbf{K}^T\Lambda)/\sqrt{d_m}$ , by introducing RBF from Eq. 7 to capture interactions between atoms.

$$\text{GeoAttention}(\mathbf{Q}, \mathbf{K}, \mathbf{V}, \Lambda) = (\mathbf{Q}\mathbf{K}^T\Lambda)/\sqrt{d_m} \cdot \mathbf{V} \quad (8)$$

The corresponding MSA is defined as follows.

$$\begin{aligned} \mathbf{H}_i^G &= \text{GeoAttention}(\mathbf{Q}_i, \mathbf{K}_i, \mathbf{V}_i, \Lambda) \quad i \in \{1, \dots, h\} \\ \text{MSA}_G(\mathbf{X}) &= \text{Concat}(\mathbf{H}_1^G, \dots, \mathbf{H}_h^G) \end{aligned} \quad (9)$$

## 4.3 Readout layer

We introduced a pooling layer at the final step, to obtain molecular properties by aggregating atom features. We applied sum-pooling and a linear layer to get the final scalar-valued predictions.

$$\hat{y} = W_{\text{pool}}\mathbf{X}^L + b, \quad (10)$$

## 4.4 Model refinement

Despite Transformer is more powerful in oversmoothing phenomenon, such works reported that the original Transformer architecture still suffers by over-smoothing problem [25, 33], resulting deeper models fails to converge. Therefore, we introduced several strategies to GeoT layers for more robust and stable convergence.

Li et al. [14] found that a graph convolution is a kind of a Laplacian smoothing on graphs. It means that a GCN plays a role in repeated smoothing which may cause undesirable and harmful effects on graph tasks, especially when the network depth is deeper. In recent days, many studies [14, 15, 16] argued that this is problematic and must be overcome, for both enhanced performance in various tasks

and richer representation learning on graphs. Several studies pointed out that the over-smoothing problem is not restricted in GNN architectures, but also exists in variants of Transformer architectures [25, 34, 33], because the self-attention is also a type of the global aggregating operation.

#### 4.4.1 AttnScale

For this reason, we adopted several strategies to minimize smoothing effect in Transformer. First, we applied *AttnScale* [25], which is developed to reduce over-smoothing effect in deep Transformer with a simple strategy.

Transformer networks with AttnScale accentuate more meaningful pattern by amplifying high-frequency signal of self-attention weights.

In specifically, AttnScale layer aims to amplify high-frequency filter aspect of attention map in order to diminish inherent low-frequency filter property [25]. Since low-frequency component of attention map as  $\mathbf{A}_{DC}^n = \frac{1}{N}\mathbf{1}\mathbf{1}^T$ , remnant considered as high-frequency term of attention map, where  $\mathbf{A}_{DC}^n$  means the direct component (DC) of an attention. AttnScale layer which scale high-frequency term by  $1 + w_a$  which is greater than one, achieves attention map preserving more HF environment of input.

$$\begin{aligned}\mathbf{A} &= \text{Attn}(\mathbf{Q}, \mathbf{K}) \\ \mathbf{A}_{DC} &= \frac{1}{N}\mathbf{1}\mathbf{1}^T \\ \mathbf{A}_{HF} &= \mathbf{A} - \mathbf{A}_{DC} \\ \text{Attn}'(\mathbf{Q}, \mathbf{K}) &= \mathbf{A}_{DC} + (1 + w_a)\mathbf{A}_{HF}\end{aligned}\tag{11}$$

In this paper, we modified AttnScale to consider our unnormalized attention map without softmax layer. Especially, we replace original low-frequency component  $\mathbf{A}_{DC}^n$  with  $\mathbf{A}_{DC}^n = \frac{1}{N}\sum_k A_{ik}^n$  to preserve the equivalence of original  $\mathbf{A}_{DC}^n$  with channel-wise average of attention map.

$$\begin{aligned}\mathbf{A}^n &= \text{Attn}_G(\mathbf{Q}, \mathbf{K}, \Lambda) \\ \mathbf{A}_{DC}^n &= \frac{1}{N}\sum_k A_{ik}^n \\ \mathbf{A}_{HF}^n &= \mathbf{A}^n - \mathbf{A}_{DC}^n \\ \text{Attn}'_G(\mathbf{Q}, \mathbf{K}, \Lambda) &= \mathbf{A}_{DC}^n + (1 + w_a^n)\mathbf{A}_{HF}^n \\ \text{GeoAttention}'(\mathbf{Q}, \mathbf{K}, \mathbf{V}, \Lambda) &= \text{Attn}'_G(\mathbf{Q}, \mathbf{K}, \Lambda) \cdot \mathbf{V}\end{aligned}\tag{12}$$

#### 4.4.2 Attention with Parallel MLP

Our second strategy modifies layer normalization scheme. We were inspired from the results of [33], which analyze the nature of MSA. Following from the above paper, we modified the network structure outside the MSA. Original Transformer encoder implements two successive layer normalizations for MSA with residual connection, and feed forward network (FFN) with residual connections, respectively, as below.

$$\begin{aligned}\widetilde{\mathbf{X}}^l &= \text{LayerNorm}(\text{MSA}_G(\mathbf{X}^l) + \mathbf{X}^l) \\ \mathbf{X}^l &= \text{LayerNorm}(\text{FFN}(\widetilde{\mathbf{X}}_i^l) + \widetilde{\mathbf{X}}_i^l)\end{aligned}\tag{13}$$

Alternatively, we modified the above equations by implementing only one layer normalization which takes MSA, FFN, and residual connection simultaneously. It can be formulated as below.

$$\mathbf{X}_i^{l+1} = \text{LayerNorm}(\text{MSA}_G(\mathbf{X}_i^l) + \text{FFN}(\mathbf{X}_i^l) + \mathbf{X}_i^l)\tag{14}$$

## 5 Experiments

### 5.1 Dataset

We evaluated our model on two benchmark datasets QM9 [35, 36] MD17 [17, 18, 19], and OC20 [37]. QM9 consists of 134k small organic molecules consist of carbon, hydrogen, nitrogen, oxygen, and fluorine in equilibrium state. All molecular conformations and their corresponding properties were created by computational simulation based on DFT calculation. Dataset contains each molecule’s stable three-dimensional coordinate and 12 scalar quantum chemical properties consist of geometric, energetic, electronic, and thermodynamic properties of given molecular structure. The task of the datasets are predicting properties from molecular conformation. Since the dataset contains comprehensive chemicals with high consistence [36], many molecular property prediction tasks were evaluated on this dataset.

The original MD17 dataset [17] consists of 10 small molecules. For each molecule, dataset contains energy and forces for different geometry with more than 10k structures, based on DFT calculation. Instead of using original dataset we used dataset consist of 1,000 training sample [19] with more precise calculation than original MD17 dataset. The task of the datasets are predicting forces and energy of given conformation, from other conformations of specific molecule.

Open Catalyst 2020 (OC20) is an open-source for learning catalysis dynamical property with chemical configuration. Similar to the benchmarks mentioned above, OC20 data consists of a three-dimensional configurations with atomic number of each adsorbate onto surfaces in the initial and DFT relaxation states. Nevertheless, OC20 is a more advanced task since the relaxed state between adsorbates and surfaces needs to be predicted the initial state thereof. OC20 includes three different types of tasks: structure to energy and forces (S2EF), initial structure to relaxed structure (IS2RS) and initial structure to relaxed energy (IS2RE) tasks. Each task is subdivided into several tasks according to dataset size. We focused on the IS2RE tasks on 10k and full sized-datasets, which needs relatively less computations.

### 5.2 Implementation

In this paper, we stacked up eight Geometry-aware Transformer layers ( $L = 8$ ) for QM9 prediction, and four ( $L = 4$ ) for MD17 and OC20 dataset. We used 300 ( $n_{basis} = 300$ ) different Gaussian functions with  $\mu_k = 0.1 \cdot k$  to embed atom-atom distances. For MLPs in RBF, We set the hidden dimension to 64 ( $d_{rbf} = 64$ ). All embedded representations ( $d_e$ ), model dimensions ( $d_m$ ) and all hidden dimensions ( $d_h$ ) of the GeoT layers were selected between (256, 512, 1,024). with (4, 16, 64) heads ( $h = 4, 16, 64$ ). We used swish activation function [38] for RBF and ELU activation function [32] for feed forward network and readout phase.

### 5.3 Training

For QM9 training, we removed 3k data which reported as structures are unstable following previous works for fair comparison [6, 7, 13, 8, 9]. Each label was trained individually. Mean absolute error (MAE) was used for evaluation according to the guidelines. Adam [39] was used as the optimizer with MAE loss and the batch size was 32 in all experiments. The learning rate was set to 0.0002 with linear warmup 3,000 steps. The learning rate decreased at 0.95 for every 200k step. We applied the early stopping method by evaluating every 10k step of training. The number of training epochs was up to 300.

To calculate forces, we assumed that the predicted energy as a function of positions  $E(\{\mathbf{r}_i\})$ . Based on the relation between force and potential energy of atoms, we calculated forces by differentiating energies with atom positions as previous works [18, 6].

$$F_j = -\frac{\partial}{\partial \mathbf{r}_j} E(\{\mathbf{r}_i\}) \quad (15)$$

In the MD17 dataset, both the energy and forces of molecular conformations are provided. To utilize both features with Eq. 15, we trained our model with the modified loss function with additional force

Table 1: Mean absolute error on QM9

Target	Unit	SchNet	PhysNet	GRAT	Cormorant	DimeNet++	GeoT
$\mu$	D	0.033	0.0529	0.03898	0.038	<b>0.0297</b>	<b>0.0297*</b>
$\alpha$	$a_0^3$	0.235	0.0615	0.07219	0.085	<b>0.0435</b>	0.05269
$\epsilon_{\text{HOMO}}$	eV	0.041	0.0329	<b>0.02228</b>	0.034	0.0246	0.0250*
$\epsilon_{\text{LUMO}}$	eV	0.034	0.0247	0.02053	0.038	<b>0.0195</b>	0.0202*
$\Delta_\epsilon$	eV	0.063	0.0425	0.035	0.061	<b>0.0326</b>	0.04392
$\langle R^2 \rangle$	$a_0^2$	<b>0.073</b>	0.765	0.76681	0.961	0.331	0.3008
$zpve$	eV	0.0017	0.0014	0.00208	0.0020	<b>0.00121</b>	0.00173*
$U_0$	eV	0.014	0.0082	0.0705	0.022	<b>0.00632</b>	0.0111
$U$	eV	0.019	0.0083	0.02825	0.021	<b>0.0062</b>	0.0117
$H$	eV	0.014	0.0084	0.02549	0.023	<b>0.0065</b>	0.0113
$G$	eV	0.014	0.0094	0.02505	0.020	<b>0.0075</b>	0.0117
$C_v$	cal/mol K	0.033	0.028	0.0326	0.026	<b>0.023</b>	0.0276

\*  $\mu$ ,  $\epsilon_{\text{HOMO}}$ ,  $\epsilon_{\text{LUMO}}$ , and  $zpve$  were evaluated on  $L = 16$ , which is different from other targets ( $L = 8$ ).

Table 2: Basis functions for ablation study

Type	Basis function
Linear basis	$a + b \cdot d_{ij}$
Gaussian basis	$\exp(-\gamma \ d_{ij} - d_k\ ^2)$
Bessel basis	$\sqrt{\frac{2}{c}} \frac{\sin(\frac{n\pi}{c}d)}{d}$

terms as Eq. 16 [18, 6].

$$L(E, \hat{E}) = |E - \hat{E}| + c \times \sum_{j=i}^n |F_j - \frac{\partial}{\partial \mathbf{r}_j} \hat{E}(\{\mathbf{r}_i\})| \quad (16)$$

Where  $c$  is a weight coefficient for the loss on forces. We set  $c$  as 1,000 in our experiments.

For training OC20 dataset, the trained model was evaluated on the in-distribution subset for validation, following the official guideline [37]. Note that we did not implement the periodic boundary condition (PBC) trick, whereas all other methods did. PBC refers the approximation technique for analysis in large system with small repeated pattern. With PBC method, multiple replica of a small unique pattern are arranged to represent a regular system. By virtue of this, broad regular surface molecules can be represented with a much smaller-sized unique cell. It significantly lowers the computations and ensures consistent representations of different atoms in same surface. We are preparing further experimental results for the next version of our manuscript.

## 6 Result

### 6.1 Model performance

We compared our result with five previous studies. Four studies [6, 8, 7, 13] are MPNN-based studies, and [9] is the only Transformer-based study. Note that all methods but SchNet [6] uses both distances and angles between atoms. Our model outperformed previous models which are only used distance between atoms. However, the performances from our model did not exceed those of DimeNet++ [13], which adopted angular information. We achieved comparable performances with DimeNet++ among six targets and outperformed for one. We achieved better performances than those from GRAT, which also adopted the Transformer architecture for QM9, except three targets.

We executed ablation studies on various types of radial basis functions. We used other two types of radial bases: Bessel basis functions, adopted in DimeNet [10, 13] and simple linear basis functions. The formula is described in 2. We also examined for linear basis function, which is most simple case of RBF. As shown in Table 3, we found that Gaussian basis functions used in our model significantly improved the model performances.

Table 3: Ablation study for basis functions in Table 2 in QM9

Target	Unit	Gaussian basis	Linear basis	Bessel basis
$\mu$	D	<b>0.0299</b>	0.664	0.0876
$\alpha$	$a_0^3$	<b>0.05269</b>	0.752	0.15
$\epsilon_{\text{HOMO}}$	eV	<b>0.02675</b>	0.0659	0.056
$\epsilon_{\text{LUMO}}$	eV	<b>0.02145</b>	0.122	0.0326
$\Delta_\epsilon$	eV	<b>0.04392</b>	0.158	0.0575
$\langle R^2 \rangle$	$a_0^2$	<b>0.3008</b>	55.4	0.3262
$zpve$	eV	<b>0.00174</b>	0.00845	0.00255
$U_0$	eV	<b>0.0111</b>	0.2026	0.0147
$U$	eV	<b>0.0117</b>	51.99	0.0275
$H$	eV	<b>0.0113</b>	0.952	0.06
$G$	eV	<b>0.0117</b>	0.574	0.013
$C_v$	cal/mol K	<b>0.0276</b>	0.195	0.06

Table 4: Force Prediction MAE in MD17

kcal/mol/A	sGDML	DimeNet	GemNet-T	GeoT	GeoT+A	GeoT+B	GeoT+C	GeoT+B+C	GeoT+A+B+C
Aspirin	0.6803	0.4981	<b>0.2191</b>	0.7081	0.7147	0.7657	0.606	<u>0.741</u>	0.721
Benzene[9]	-	0.1868	0.1453	-	0.10879	0.109	0.1132	0.1206	<b>0.0978</b>
Ethanol	0.3298	0.2306	0.0853	0.09494	0.093508	0.08967	0.0952	<b>0.07741</b>	0.08599
Malonaldehyde	0.4105	0.3828	0.1545	<b>0.13985</b>	-	0.1408	0.14215	0.1476	0.151
Naphthalene	0.1107	0.2145	<b>0.0553</b>	0.2198	0.2264	0.1947	0.2321	0.1949	<u>0.1924</u>
SalicylicAcid	0.2790	0.3736	<b>0.1268</b>	0.2869	0.289	0.2849	0.2758	0.2755	<u>0.2667</u>
Toluene	0.1407	0.2168	<b>0.0600</b>	0.1541	0.1538	<u>0.1307</u>	0.1642	0.1403	0.147
Uracil	0.2398	0.3021	<b>0.0969</b>	0.1471	0.1499	<u>0.1341</u>	0.1631	0.13097	<u>0.1285</u>

A means that the use of atom-aware two-body kernel, which is described in Eq. 7), otherwise, Eq. 6 was used instead. B and C are the use of Paralleled MLP and the AttnScale, respectively.

The performance from MD17 is described in Table 4. We compared our results with previously reported methods [18, 10, 20]. GeoT achieved the best performance in three molecules, whereas GemNet-T outperformed in the rest five molecules. Note that DimeNet uses angle and GemNet-T uses torsional angle features in a molecule. We did another ablation study with two types of model refinements mentioned above and the existence of atom embeddings. The model refinements improved the model performance in six out of eight types of molecules, except for Aspirin and Malonaldehyde.

Table 5 and 6 showed the performances of OC20 IS2RE task of 10k and full datasets. The baseline results of [6, 10, 40, 13] were retrieved from the open leaderboard. We figured out that implementing PBC clearly improves the model performance in SchNet. Without PBC, SchNet does not exceed our model in both of the tasks. The model refinements did not effective in 10k task. We remain the issue with open question.

## 6.2 Attention map visualization

We visualized attention maps from the trained model to analyze the behavior of our attention mechanism. First, we will describe how we extract attention values. Next, we will discuss two subjects in this section, the aspects of attentions and the effects of model refinements.

Different from the previous work [41], we extracted  $\| \text{Attn}'_G(\mathbf{Q}, \mathbf{K}, \mathbf{\Lambda}) \|_2$  of several molecules from the trained model. We picked a query atom  $i$  of each molecule, and visualized attention values with another atom  $j$ . Query atoms are marked with red asterisk, and attention norms of key atom  $j$  from the query atom  $i$  are colored with blue shades.

The attention values in GeoT are differ from the original Transformer in two points. First, GeoT updates each atom representation with *unnormalized* attention scale, given by Eq. 8. Second,  $\text{Attn}'_G$  includes a novel feature  $\mathbf{\Lambda}$ , which endows a geometric feature with the attention. By capturing

Table 5: In-distribution validation energy MAE for OC20 IS2RE 10k task

model	MAE
SchNet*	1.059
SchNet (without PBC)	1.077
DimeNet*	1.0117
CGCNN*	0.9881
DimeNet++*	<b>0.8837</b>
GeoT	<u>0.9631</u>
GeoT + Atom aware kernel	0.996
GeoT + ParallelMLP	0.966
GeoT + AttnScale	1.018
GeoT + Attnscale + ParallelMLP	1.0516
GeoT + Attnscale + ParallelMLP + Atom aware kernel	0.9786

The results with \* were retrieved from [37]. Note that we did not implement PBC conditions into GeoT, while other methods adopted it.

Table 6: In-distribution validation energy MAE for OC20 IS2RE full task

model	MAE
SchNet	0.6458
SchNet (without PBC)	0.729
GeoT (without PBC)	0.7002

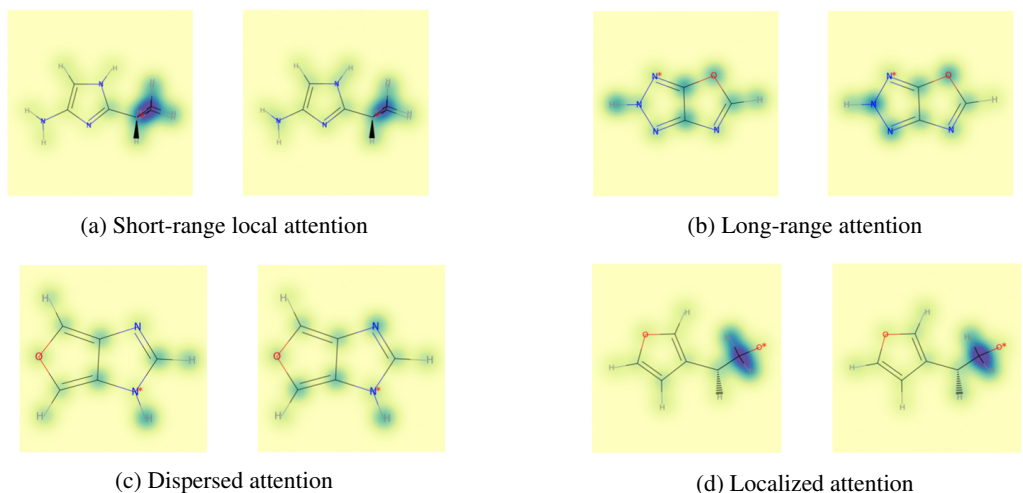


Figure 3: The four sample pairs of the attention map of QM9 model. Each pair is retrieved from the Second (left) and Seventh GeoT layer (right), respectively. The red asterisk is the arbitrarily selected query atom of a given molecule. The attention maps varies according to molecule types. (a) and (b) are the examples of short-range and long-range attention from query atom, respectively. (c) and (d) are the distributed and localized attention, respectively. All model is trained on HOMO.



## 7 Discussion

Based on the above results and visualizations, we discuss several issues on the behavior of GeoT with multiple aspects.

### Q1. Is Transformer better than message-passing for molecular graph representation?

The most significant difference is that the ability of learning representation between any two atoms in a molecule. In MPNN, messages are only passed to closely located atoms limited to cutoff values. However, the attention mechanism (both of the original self-attention and GeoAttention) acts globally in a molecule so that any two atom configuration can contribute to the whole molecule representation learning.

Second, the deep message-passing models often suffer from the over-smoothing problem, while Transformer-based networks showed outstanding performances in various tasks with deeper structures.

### Q2. Is GeoAttention better than the original self-attention for molecular graph representation?

We emphasize that GeoAttention includes a radial-basis feature  $\Lambda$  for atom pair distances and removes a softmax function. First,  $\Lambda$  provides all pairwise atom-atom distances with multiple bases. We assumed that if all atom-atom pairs with their distances from all combinations are available, then the model can recover the global view of its three-dimensional configurations. Second, the scale of GeoAttention is not normalized so that it is not related with the number of atoms.

Note that we do not use either message passing framework or graph convolution in our method. Therefore, our proposed model can capture the global perspective of a molecular conformation without any local restriction. In addition, our method is relatively free from over-smoothing problems regardless of the model depth with additional refinements.

**Q3. What insights can we derive from the attention map based on GeoAttention?** The attention visualization provides deeper insights than the prediction performance only, because we can investigate each atom and their relations in each molecule. The attention maps showed that the nature of atom-atom interaction and the aromaticity are properly reflected. Further, it can suggest unknown chemical interactions in complex system, which can be a significant clue of synthetic chemistry researches.

## 8 Conclusion

In this study, we introduced geometry-aware attention which can capture interactions regardless of distances. We added geometric information by adopting self-attentions of the distance representations between atoms with the RBF. We evaluated our model on QM9 and MD17. Our model outperformed previous works based on distances and comparable with state-of-the-art models which utilized additional angular information. We also studied on the candidates of the RBF, and showed Gaussian basis function performed significantly better than other functions. We also displayed attention weights, which supported our assumption that model can attend atom pairs located far from each other. We argue that our model achieved that long-range interactions between any intramolecular atom pairs, which cannot be available for previous methods using the restricted convolutional filters. We will explore additional geometric features to improve our model performance. In the future, we will explore more extensive experiments on OC20, including PBC and more variable tasks.

## References

- [1] Matthias Rupp, Alexandre Tkatchenko, Klaus-Robert Müller, and O Anatole Von Lilienfeld. Fast and accurate modeling of molecular atomization energies with machine learning. *Physical review letters*, 108(5):058301, 2012.
- [2] Sönke Lorenz, Axel Groß, and Matthias Scheffler. Representing high-dimensional potential-energy surfaces for reactions at surfaces by neural networks. *Chemical Physics Letters*, 395(4-6):210–215, 2004.
- [3] Jörg Behler and Michele Parrinello. Generalized neural-network representation of high-dimensional potential-energy surfaces. *Physical review letters*, 98(14):146401, 2007.

- [4] Albert P Bartók, Mike C Payne, Risi Kondor, and Gábor Csányi. Gaussian approximation potentials: The accuracy of quantum mechanics, without the electrons. *Physical review letters*, 104(13):136403, 2010.
- [5] David Duvenaud, Dougal Maclaurin, Jorge Aguilera-Iparraguirre, Rafael Gómez-Bombarelli, Timothy Hirzel, Alán Aspuru-Guzik, and Ryan P Adams. Convolutional networks on graphs for learning molecular fingerprints. *arXiv preprint arXiv:1509.09292*, 2015.
- [6] Kristof T Schütt, Pieter-Jan Kindermans, Huziel E Sauceda, Stefan Chmiela, Alexandre Tkatchenko, and Klaus-Robert Müller. Schnet: A continuous-filter convolutional neural network for modeling quantum interactions. *arXiv preprint arXiv:1706.08566*, 2017.
- [7] Oliver T Unke and Markus Meuwly. Physnet: A neural network for predicting energies, forces, dipole moments, and partial charges. *Journal of chemical theory and computation*, 15(6):3678–3693, 2019.
- [8] Brandon Anderson, Truong-Son Hy, and Risi Kondor. Cormorant: Covariant molecular neural networks. *arXiv preprint arXiv:1906.04015*, 2019.
- [9] Sanghyun Yoo, Young-Seok Kim, Kang Hyun Lee, Kuhwan Jeong, Junhwi Choi, Hoshik Lee, and Young Sang Choi. Graph-aware transformer: Is attention all graphs need? *arXiv preprint arXiv:2006.05213*, 2020.
- [10] Johannes Klicpera, Janek Groß, and Stephan Günnemann. Directional message passing for molecular graphs. *arXiv preprint arXiv:2003.03123*, 2020.
- [11] Yoni Choukroun and Lior Wolf. Geometric transformer for end-to-end molecule properties prediction. *arXiv preprint arXiv:2110.13721*, 2021.
- [12] Justin Gilmer, Samuel S Schoenholz, Patrick F Riley, Oriol Vinyals, and George E Dahl. Neural message passing for quantum chemistry. In *International Conference on Machine Learning*, pages 1263–1272. PMLR, 2017.
- [13] Johannes Klicpera, Shankari Giri, Johannes T. Margraf, and Stephan Günnemann. Fast and uncertainty-aware directional message passing for non-equilibrium molecules. In *NeurIPS-W*, 2020.
- [14] Qimai Li, Zhichao Han, and Xiao-Ming Wu. Deeper insights into graph convolutional networks for semi-supervised learning. In *Proceedings of the AAAI Conference on Artificial Intelligence*, volume 32, 2018.
- [15] Deli Chen, Yankai Lin, Wei Li, Peng Li, Jie Zhou, and Xu Sun. Measuring and relieving the over-smoothing problem for graph neural networks from the topological view. In *Proceedings of the AAAI Conference on Artificial Intelligence*, volume 34, pages 3438–3445, 2020.
- [16] Wenbing Huang, Yu Rong, Tingyang Xu, Fuchun Sun, and Junzhou Huang. Tackling over-smoothing for general graph convolutional networks. *arXiv preprint arXiv:2008.09864*, 2020.
- [17] Stefan Chmiela, Alexandre Tkatchenko, Huziel E Sauceda, Igor Poltavsky, Kristof T Schütt, and Klaus-Robert Müller. Machine learning of accurate energy-conserving molecular force fields. *Science advances*, 3(5):e1603015, 2017.
- [18] Stefan Chmiela, Huziel E Sauceda, Igor Poltavsky, Klaus-Robert Müller, and Alexandre Tkatchenko. sgdmf: Constructing accurate and data efficient molecular force fields using machine learning. *Computer Physics Communications*, 240:38–45, 2019.
- [19] Stefan Chmiela, Huziel E Sauceda, Klaus-Robert Müller, and Alexandre Tkatchenko. Towards exact molecular dynamics simulations with machine-learned force fields. *Nature communications*, 9(1):1–10, 2018.
- [20] Johannes Gasteiger, Florian Becker, and Stephan Günnemann. Gemnet: Universal directional graph neural networks for molecules. *Advances in Neural Information Processing Systems*, 34:6790–6802, 2021.
- [21] Yi Liu, Limei Wang, Meng Liu, Yuchao Lin, Xuan Zhang, Bora Oztekin, and Shuiwang Ji. Spherical message passing for 3d molecular graphs. In *International Conference on Learning Representations*, 2022.
- [22] Nathaniel Thomas, Tess Smidt, Steven Kearnes, Lusann Yang, Li Li, Kai Kohlhoff, and Patrick Riley. Tensor field networks: Rotation-and translation-equivariant neural networks for 3d point clouds. *arXiv preprint arXiv:1802.08219*, 2018.

- [23] Fabian B Fuchs, Daniel E Worrall, Volker Fischer, and Max Welling. Se (3)-transformers: 3d roto-translation equivariant attention networks. *arXiv preprint arXiv:2006.10503*, 2020.
- [24] Ashish Vaswani, Noam Shazeer, Niki Parmar, Jakob Uszkoreit, Llion Jones, Aidan N Gomez, Lukasz Kaiser, and Illia Polosukhin. Attention is all you need. *arXiv preprint arXiv:1706.03762*, 2017.
- [25] Peihao Wang, Wenqing Zheng, Tianlong Chen, and Zhangyang Wang. Anti-oversmoothing in deep vision transformers via the fourier domain analysis: From theory to practice. *arXiv preprint arXiv:2203.05962*, 2022.
- [26] Sheng Wang, Yuzhi Guo, Yuhong Wang, Hongmao Sun, and Junzhou Huang. Smiles-bert: large scale unsupervised pre-training for molecular property prediction. In *Proceedings of the 10th ACM international conference on bioinformatics, computational biology and health informatics*, pages 429–436, 2019.
- [27] Łukasz Maziarka, Tomasz Danel, Sławomir Mucha, Krzysztof Rataj, Jacek Tabor, and Stanisław Jastrzębski. Molecule attention transformer. *arXiv preprint arXiv:2002.08264*, 2020.
- [28] Yu Rong, Yatao Bian, Tingyang Xu, Weiyang Xie, Ying Wei, Wenbing Huang, and Junzhou Huang. Self-supervised graph transformer on large-scale molecular data. *Advances in Neural Information Processing Systems*, 33:12559–12571, 2020.
- [29] Chengxuan Ying, Tianle Cai, Shengjie Luo, Shuxin Zheng, Guolin Ke, Di He, Yanming Shen, and Tie-Yan Liu. Do transformers really perform badly for graph representation? *Advances in Neural Information Processing Systems*, 34:28877–28888, 2021.
- [30] Dexiong Chen, Leslie O’Bray, and Karsten Borgwardt. Structure-aware transformer for graph representation learning. In *International Conference on Machine Learning*, pages 3469–3489. PMLR, 2022.
- [31] Jimmy Lei Ba, Jamie Ryan Kiros, and Geoffrey E Hinton. Layer normalization. *arXiv preprint arXiv:1607.06450*, 2016.
- [32] Djork-Arné Clevert, Thomas Unterthiner, and Sepp Hochreiter. Fast and accurate deep network learning by exponential linear units (elus). *arXiv preprint arXiv:1511.07289*, 2015.
- [33] Namuk Park and Songkuk Kim. How do vision transformers work? *arXiv preprint arXiv:2202.06709*, 2022.
- [34] Han Shi, Jiahui Gao, Hang Xu, Xiaodan Liang, Zhenguo Li, Lingpeng Kong, Stephen Lee, and James T Kwok. Revisiting over-smoothing in bert from the perspective of graph. *International Conference on Learning Representations*, 2022.
- [35] Lars Ruddigkeit, Ruud Van Deursen, Lorenz C Blum, and Jean-Louis Reymond. Enumeration of 166 billion organic small molecules in the chemical universe database gdb-17. *Journal of chemical information and modeling*, 52(11):2864–2875, 2012.
- [36] Raghunathan Ramakrishnan, Pavlo O Dral, Matthias Rupp, and O Anatole von Lilienfeld. Quantum chemistry structures and properties of 134 kilo molecules. *Scientific Data*, 1, 2014.
- [37] Lowik Chanussot\*, Abhishek Das\*, Siddharth Goyal\*, Thibaut Lavril\*, Muhammed Shuaibi\*, Morgane Riviere, Kevin Tran, Javier Heras-Domingo, Caleb Ho, Weihua Hu, Aini Palizhati, Anuroop Sriram, Brandon Wood, Junwoong Yoon, Devi Parikh, C. Lawrence Zitnick, and Zachary Ulissi. Open catalyst 2020 (oc20) dataset and community challenges. *ACS Catalysis*, 2021.
- [38] Prajit Ramachandran, Barret Zoph, and Quoc V Le. Searching for activation functions. *arXiv preprint arXiv:1710.05941*, 2017.
- [39] Diederik P Kingma and Jimmy Ba. Adam: A method for stochastic optimization. *arXiv preprint arXiv:1412.6980*, 2014.
- [40] Tian Xie and Jeffrey C Grossman. Crystal graph convolutional neural networks for an accurate and interpretable prediction of material properties. *Physical review letters*, 120(14):145301, 2018.
- [41] Jesse Vig. A multiscale visualization of attention in the transformer model. In *Proceedings of the 57th Annual Meeting of the Association for Computational Linguistics: System Demonstrations*, pages 37–42, Florence, Italy, July 2019. Association for Computational Linguistics.